

Radiographic Technique for Densitometric Studies Using Heavy Ion Microbeams

J. Muscio^(a), H. Somacal^(a,b), A. A. Burlon^(a,b), M. E. Debray^(a,b), A. J. Kreiner^(a,b,c),
J. M. Kesque^(b), D. M. Minsky^(b) and A. A. Valda^(a,b), M. Davidson^(b,c), and J.
Davidson^(b,c)

^(a) ECyT, UNSAM, 1650 San Martín, Buenos Aires, Argentina

^(b) U.A.Física, Laboratorio TANDAR, CNEA, 1650 San Martín, Buenos Aires, Argentina

^(c) CONICET, Argentina

Abstract. Different analytical techniques are typically used to perform multi-elemental and densitometric analysis by means of particle beams with micrometric spatial resolution. Usually, those analyses are respectively performed by PIXE and STIM. Traditionally, to characterize the trace element concentrations in a specimen two different experiments are required with differences in setups and types of detectors employed, as well as in the necessary ion current intensities. In this work, we discuss the latest results in the development of a new technique that synthesizes both analyses in just a single one, by means of heavy ion induced x-ray emission. This technique, implemented for the first time at the Tandara Laboratory, employs a second target in addition to the sample under study. The multi-elemental information of the specimen is provided by its PIXE signal and its densitometric information is supplied by the PIXE signal of the secondary target, which is placed immediately behind the sample under analysis. These PIXE signals are produced and acquired during the same experiment, allowing the analysis of both features (composition and density) at the same time. The X-rays originated in the secondary target are attenuated when traversing the specimen in the direction of the detector and consequently a radiographic image of the specimen is obtained. In this case, the characteristic X-rays of the secondary target act like a monochromatic secondary source. In the present work, a method to estimate the thickness of specimens is introduced and compared with estimations performed by the STIM method.

Keywords: Microprobe, PIXE, STIM, Radiography, Heavy Ions.

INTRODUCTION

Particle microprobes are well established devices and widely used around the world to characterize materials. In particular, a microprobe was recently installed at the Tandara Accelerator of the Argentine Atomic Energy Commission [1]. At present, two techniques associated with the microprobe were implemented. One is micro-PIXE [2] that combines the standard PIXE (Particle Induced X-ray Emission) technique, with a focused heavy ion microbeam, to determine the microdistribution of trace elements in a sample. The other technique is STIM (Scanning Transmission Ion Microscopy) [3] that consists in the measurement of the energy loss of the ions transmitted through the sample. This technique is applied to density studies in materials, analyzing the ion energy loss when traversing a sample. Both techniques have

high spatial resolution provided by ion beams of micrometer dimensions. For a quantitative characterization of trace elements, it is necessary to use both techniques for a given sample. This is cumbersome, because it requires two independent experiments. PIXE needs high currents ($\sim 10^6$ particles/sec) to enhance the production induced of X-rays while STIM requires low currents (~ 200 particles/sec) to protect the Si surface barrier detector. It is well known that the X-ray production cross section is larger with heavy-ions than protons [4]. This advantage allowed the development of a new technique to perform densitometric and multielemental analysis of samples simultaneously using only one detector [5]. The densitometry aspect of this technique utilizes the differential absorption of the induced characteristic X-rays in a secondary target placed immediately behind the specimen. This target,

properly selected, acts like a monochromatic secondary source of photons. Thus, the photons induced in the sample allow the multielemental analysis (PIXE spectrometry) and, on the other hand, the X-rays induced in the secondary target allow us to obtain the sample density (X-ray densitometry). The latter X-ray intensity is attenuated while traversing the specimen. A first experimental test, obtained with the Tandar microprobe and an ^{16}O beam at 50 MeV, was performed using a Cu target and Fe as a secondary target, as shown in fig. 1. The same conditions were assumed to calculate the simulated profiles. This figure compares experimental and simulated PIXE spectra of the sample (left hand side) and of the secondary target (right hand side). A somewhat related procedure, but only for imaging purposes, has been proposed in ref. [6].

As just discussed, a method to estimate the local thickness of specimens is introduced here and additionally compared with results obtained by simulating STIM. It should be mentioned that both STIM and the method proposed here have to deal with the complexities associated with the sample matrix.

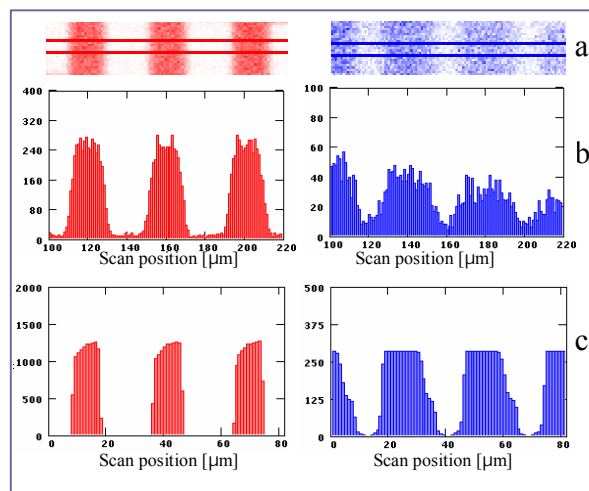


FIGURE 1. a) Experimental maps of a Cu target sample (left) and of a secondary Fe target (right). Horizontal lines in both maps exhibit the gates, which are used to extract the experimental profiles shown below. b) Experimental profiles of Cu (left) and Fe (right). c) Simulated profiles of Cu (left) and Fe (right) in arbitrary units.

NUMERICAL SIMULATIONS

To understand the processes that take place in this type of radiography, simulations considering a sample constituted by equidistant vertical bars of copper and a Fe standard, placed immediately behind the sample, were performed using similar conditions to the

experimental ones. The X-ray yields at different energies were calculated with the computer program Inner Shell Ionization Cross Sections (ISICS) [7].

The set-up adopted for the numerical simulations is shown in fig. 2. The thick target considered in these simulations consists in a group of separated Cu bars. The total X-ray yield from this target, following ^{16}O bombardment, has been calculated as the sum of yields of a succession of thin layers. The measured X-ray intensity from each thin homogeneous layer depends on the quantity of ions crossing that layer, the ionization cross section, the branching ratio, the fluorescent yield and the X-ray detection efficiency [2].

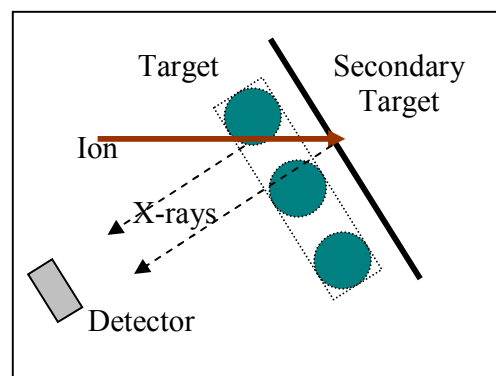


FIGURE 2. Scheme of the arrangement (equal to the experimental one) used for the numerical simulations. The circles represent cross sections of the thick Cu bars used.

The use of a thick sample implies that the intensity attenuation in the same material must be considered. For a layer of the sample, at a depth D from the surface, the X-ray intensity is attenuated by $\exp(-\mu(E_X) \cdot D)$, where $\mu(E_X)$ is the average linear attenuation coefficient (cm^{-1}) for a photon of energy E_X in the material and D is the distance (cm) that such photon must travel, in the material, before escaping towards the detector. In addition to this, the presence of the secondary target suggests the possibility of radiography. This means that the X-rays induced in the secondary target are attenuated when traversing the sample in the direction of the detector and consequently a radiographic image of the specimen is obtained. This feature is used to estimate the sample density.

Two possible methods have been studied to estimate the density of the target. One is an iterative method, whereas the other is a differential attenuation method. Both methods require a previous calibration step in which the characteristic X-ray production by heavy ion bombardment must be measured.

Iterative Method

The iterative method compares the estimated intensity of X-rays attenuated by a thin layer, with the intensity of X-rays measured.

In this evaluation, the decreasing production of X-rays induced by the lower-energy ions after traversing the thick target has been considered. The experimental determination would have to be done by interpolating the measured X-ray production cross sections, but in this case, it was determined numerically.

This comparison is repeated successively with an increasing number of thin layers until the calculated and measured intensities get to be equal. Then, when the iterative process is finished, the accumulated thickness is identified with the actual thickness.

Differential Attenuation Method

The differential attenuation method consists in the determination of the thickness of the target, using the different attenuations that are experienced by X-rays of different energies, when traversing a thickness of a given material.

The discrete spectrum (K-series or L-series) induced in the secondary target is attenuated in a different way by a given specimen. This fact is due to the different average linear attenuation coefficient for different energies. Therefore, the discrete spectrum suggests the use of the difference in the X-ray attenuations, for different energies, for determining the density of the specimen. The use of the K-series or the L-series depends on the sample at study.

It is possible to see that the ratio between the K_α and K_β X-ray intensities, which emerge from the secondary target, is (approximately) independent of the projectile energy. Even if the X-ray yield diminishes with the energy of the incident ions, the ratio between K_α and K_β intensities is independent of this energy and is given in equation 1.

$$K_{\alpha\beta} = \frac{I_0(K_\alpha)}{I_0(K_\beta)} = \frac{I(K_\alpha)}{I(K_\beta)} \quad (1)$$

Where I represent the intensities ($K_{\alpha(\beta)}$) and the subscript 0 corresponds to the case when the ions impact directly on the secondary target without traversing the sample previously. Considering the differential attenuation, it is possible to see, as shown in equation 2 that the sample thickness is:

$$\delta_s = \frac{\ln\left(\frac{K_{\alpha\beta}^{\text{det}}}{K_{\alpha\beta}}\right)}{\mu_s^\beta - \mu_s^\alpha} \quad (2)$$

$K_{\alpha\beta}^{\text{det}}$ represents the ratio between the detected intensities ($K_{\alpha\beta}$) i.e. the relation after attenuation in the sample, whereas $K_{\alpha\beta}$ is the relation without attenuation, which can be measured in the calibration experiment and $\mu_s^{\alpha(\beta)}$ indicates the average linear attenuation coefficient (cm^{-1}) for $K_\alpha(K_\beta)$ photons of the secondary target as they traverse the sample.

RESULTS

Fig. 3 shows a profile reconstructed with the differential attenuation method compared to the actual geometric sample profile (solid bars) and the STIM profile that is superimposed to it. The reconstructed curves show an overestimation because they are not corrected by the solid angle to the detector. This effect is characteristic in radiography when the object is neighboring to the source and can be corrected. In this case, the sample orientation is perpendicular to the incident beam.

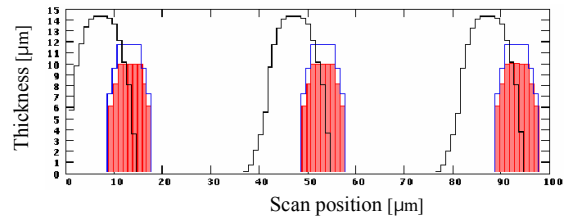


FIGURE 3. The profile reconstructed from numerical simulations with the differential attenuation method is compared with a STIM reconstruction. The solid bars represent the geometric contour of the sample and STIM data correspond to the curve superimposed to the sample profile. The curve that shows an overestimation, a broadening and a shift to the left hand side on the figure corresponds to the differential attenuation reconstruction without geometric corrections.

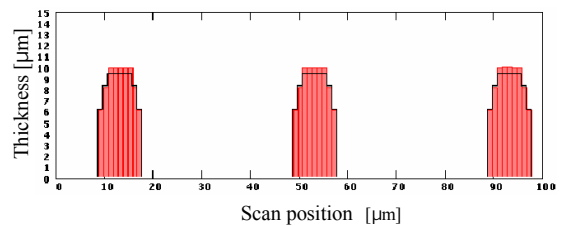


FIGURE 4. Profile reconstructed with the iterative method, from numerical simulations. The solid bar represents the geometric contour of the sample and the reconstructed data correspond to the curve superimposed to the sample profile.

Fig. 4 shows a profile reconstructed with the iterative method compared to the geometric profile of the sample (solid bars). The reconstructed curves show good agreement with the sample profile.

An additional recent experiment using focused 50-MeV $^{16}\text{O}^{+5}$ ions provided also by the 20-MV van de Graaf accelerator at the Tandem Laboratory was carried out and biological tissue samples were investigated. During approximately 20-min the samples were irradiated by 10-pA beams with spot sizes of $4 \times 4 \text{ }\mu\text{m}^2$. The experimental arrangement is shown in fig. 2 with the X-ray detector placed at 135° to the beam direction. A high-resolution X-ray detector (70-eV at 1-keV) liquid-Nitrogen-cooled, thin-windowed, Si(Li) counter (active area of 30-mm^2 , 3-mm thickness) was used. The measurement was performed in two steps: first the system was calibrated with a thin $47.6(\pm 75\%)\text{-}\mu\text{g}/\text{cm}^2$ Ti standard, placed at the same position as the samples; second the PIXE and radiography data were obtained using the Ti standard placed immediately behind the specimen. The measurements were made on $150 \times 80\text{-}\mu\text{m}^2$ regions and PIXE spectra and maps were recorded event by event (see fig. 5).

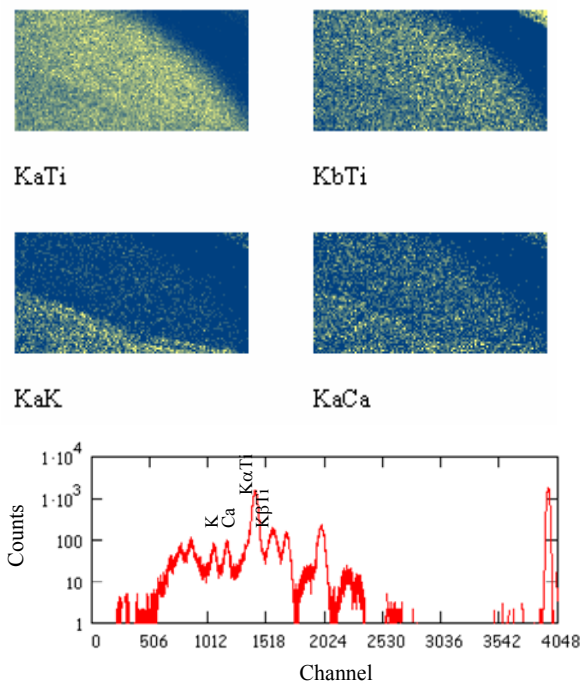


FIGURE 5. Experimental data of a Ti secondary target. Maps of K(K_α) and Ca(K_α) induced in the biological sample and maps associated to Ti K_α , K_β lines. A total PIXE spectrum is shown at the bottom.

The sample, showed here, was obtained from precancerous tissue [1]; it was cut in $10\text{-}\mu\text{m}$ thick sections with a cryomicrotome and mounted on a $0.15\text{-}\mu\text{m}$ ultrapure polycarbonate backing and freeze-

dried. Fig. 5 shows on top, Ti K_α and K_β maps of the secondary target used and in the middle part, K and Ca K_α -maps, induced in the sample. At the bottom, the total PIXE spectrum is shown on which the lines “producing” the maps are indicated. In spite of the low statistics, differences in production and attenuation of the Ti lines start to appear.

DISCUSSION

The technique presented here is dependent on a suitable selection of the secondary target to be combined with the sample under study (to avoid masking the trace elements). The obtained results encourage further studies on the selection of appropriate secondary targets. Moreover, preliminary results concerning densitometric imaging based on the L or M-lines of medium and high Z elements appear as a useful tool. At present, we are studying different secondary targets to be used in experiments with histology sections. A systematic measurement of production cross-sections as functions of projectile energy, for different materials to be used as secondary targets, is needed to make further progress.

REFERENCES

1. P. Stoliar, A. J. Kreiner, M. E. Debray, M. E. Caraballo, A. A. Valda, J. Davidson, M. Davidson, J. M. Kesque, H. Somacal, H. Di Paolo, A. A. Burlon, M. J. Ozafran, M. E. Vazquez, D. Minsky, E. M. Heber, V. A. Trivillin, A. E. Schwint. *Applied Radiation and Isotopes* 61 (2004) 771.
2. G. W. Grime, F. Watt and J. A. Cookson, “Analytical Techniques” in *Principles and Applications of High-Energy Ion Microbeams*, edited by F. Watt and G. W. Grime, Dep. of Nucl. Phys. University of Oxford, 1987, pp. 21-43.
3. M. B. H. Breese, J. P. Landsberg, P. J. C. King, G. W. Grime, F. Watt, *Nucl. Instr. and Meth. B*64 (1992) 505-511.
4. M. J. Ozafran, M.E.Debray, R. Eusebi, A.J.Kreiner, M.E.Vázquez, A.A.Burlón, P.Stoliar. *Nucl. Instr. And Meth. in Phys. Res.B* 201(2003)317-324.
5. J. Muscio, H. Somacal, A. Burlon, M. Debray, A.J.Kreiner, J.M.Kesque, D.Minsky, A.Valda. “A radiographic technique with heavy ion microbeams” in VI Latin-American Symposium of Nuclear Physics and Applications-2005, ed. by O. Civitarese, et al., AIP Conference Proceedings, 2007, Volume 884, pp. 479-481.
6. K. Ishii, S. Matsuyama, Y. Watanabe, Y. Kawamura, T. Yamaguchi, R. Oyama, G. Momose, A. Ishizaki, H. Yamazaki, Y. Kikuchi, *Nucl. Instr. and Meth. A*571 (2007) p. 64.
7. Z. Liu and S.J. Cipolla, *Comp. Phys. Comm.* 97 (1996), p. 315.